RESEARCH ARTICLE

Layered group-IV-V-VI semiconductors with superior piezoelectricity and ferroelectricity

Lixin Zhou[1], Yu Guo[1, †], Yan Su[1], Jijun Zhao[2, 3]

1 Key Laboratory of Materials Modification by Laser, Ion and Electron Beams (Dalian University of Technology), Ministry of Education, Dalian 116024, China

2 Guangdong Provincial Key 2 Laboratory of Quantum Engineering and Quantum Materials, School of Physics, South China Normal University, Guangzhou 510006, China

3 Guangdong-Hong Kong Joint Laboratory of Quantum Matter, Frontier Research Institute for Physics, South China Normal University, Guangzhou 510006, China

Corresponding author. E-mail: †guoyu_dlut@dlut.edu.cn

Received August 26, 2025; accepted December 28, 2025

Supplementary Material

S1. Various stacking configurations of bilayer SnP_2Se_6

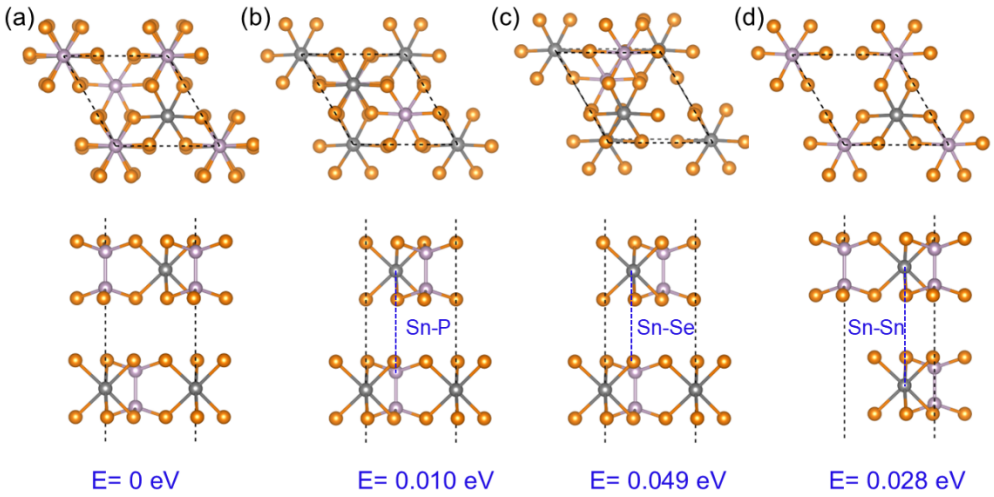

Fig. S1 Various stacking configurations of bilayer SnP_2Se_6. (a-d) correspond to configurations where the upper Sn atom is positioned over a vacancy, and over P, Se, and Sn atoms in the lower layer, respectively. Taking the structure in (a) as the reference (0 eV), the other three stacking configurations have higher energies.

S2. Various stacking configurations of bilayer SnP_2Se_6

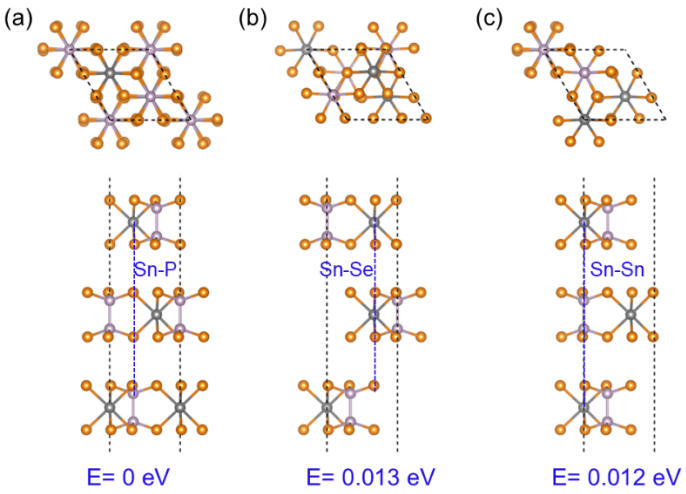

Fig. S2. Various stacking configurations of trilayer SnP_2Se_6. (a-c) correspond to configurations where the upper Sn atom is positioned over P, Se, and Sn atoms in the lower layer, respectively. Taking the structure in (a) as the reference (0 eV), the other stacking configurations have higher energies.

S3. Thermodynamic Stability of monolayer SnP_2Se_6

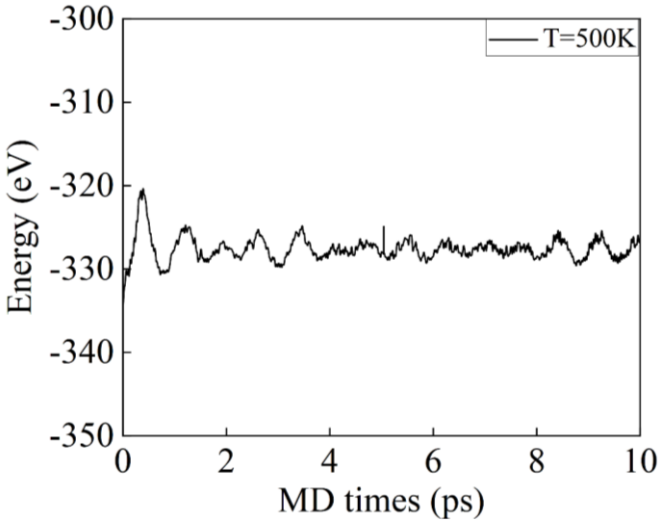

Fig. S3. Variations of energy with the time of AIMD simulation for the monolayer SnP_2Se_6 with temperature controlled at 300 K.

S4. AIMD simulations of O_2 collision with SnP_2Se_6 monolayer at 300 K

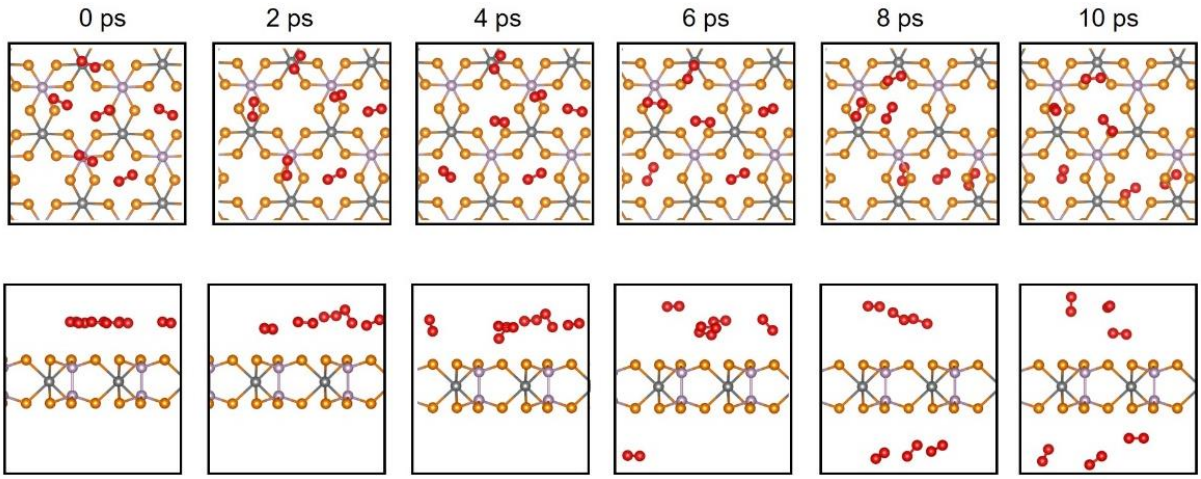

Fig. S4. Snapshots of AIMD simulations of O_2 oxidation at 300 K at 2 -10 ps. It can be seen that O_2 molecules are typically bounced back to the vacuum after collision with the SnP_2Se_6 monolayer. Hence, it seems that SnP_2Se_6 monolayer exhibits superior oxidation resistance.

S5. Adsorption structure of water on group-IV-V-VI monolayer surface

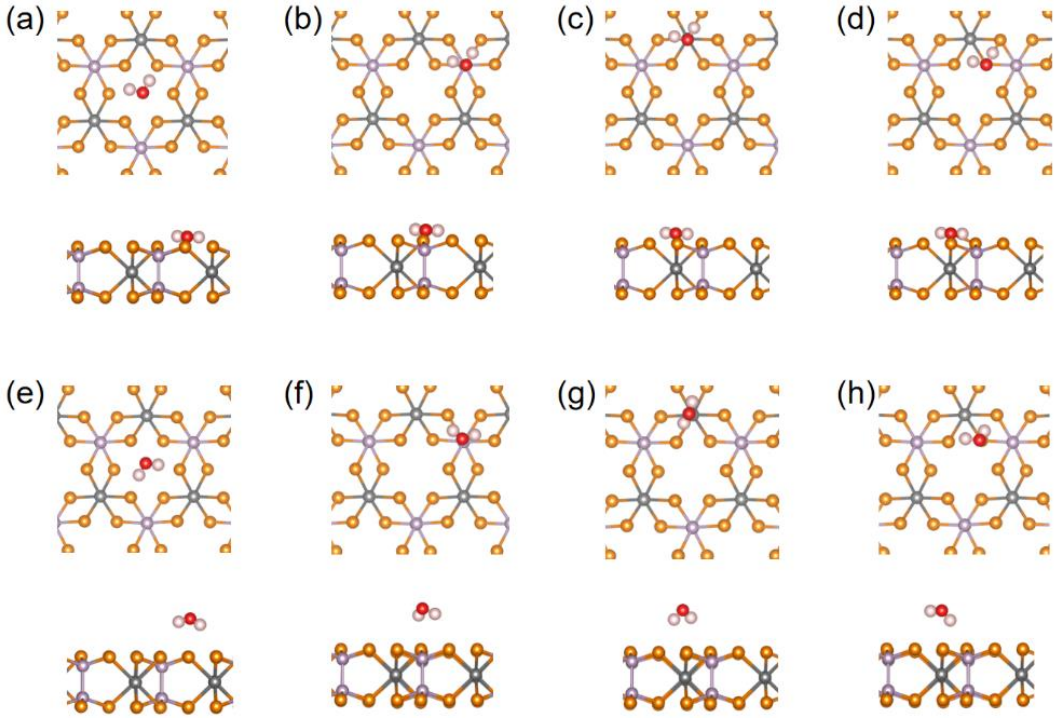

Fig. S5. (a-d) show the pre-optimization structures with the water molecule placed at four inequivalent adsorption sites on the SnP_2Se_6 surface: the center of a hexagonal ring and the top sites of three different atoms; (e-h) show the post-optimization structures, where all atomic distances are greater than 2.5 Å.

S6. Phonon dispersions of group-IV-V-VI monolayers

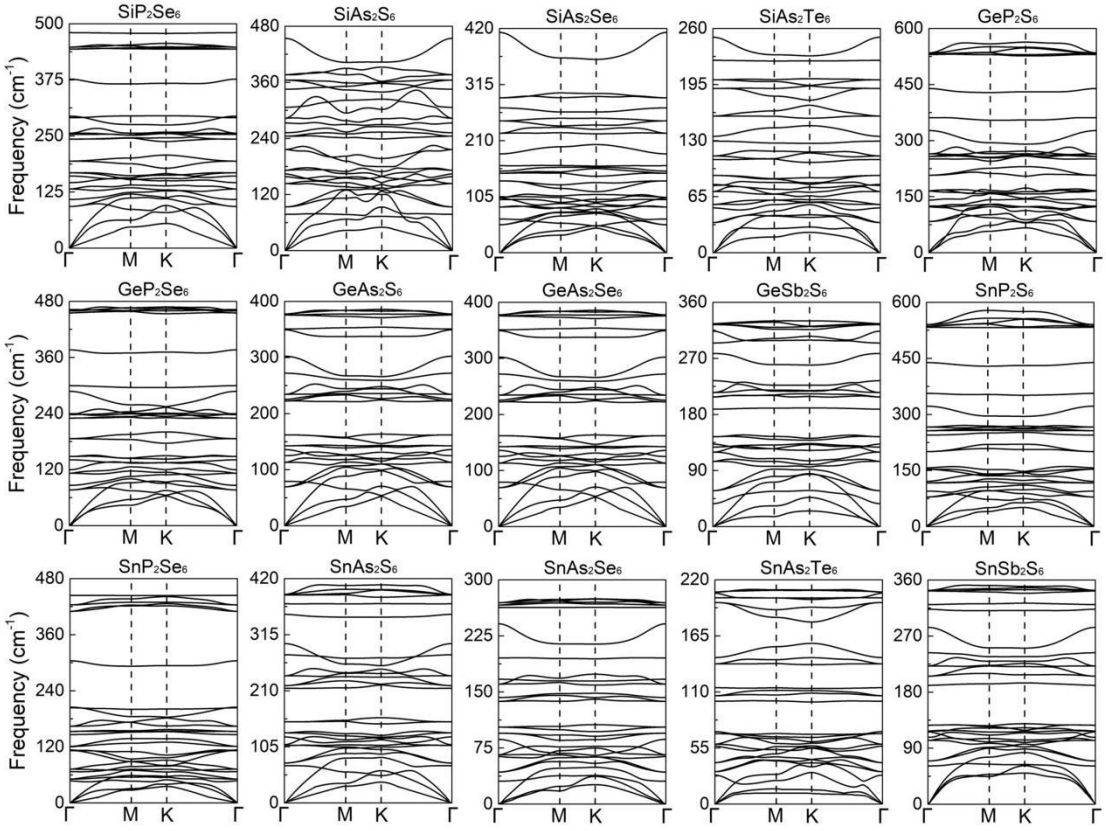

Fig. S6. Phonon dispersions of group-IV-V-VI monolayers.

S7. Elastic constants for the group-IV-V-VI monolayers

Table S1. Elastic constants for the group-IV-V-VI monolayers.

Materials	C_{11}	C_{12}	C_{13}	C_{14}	C_{33}	C_{44}
SiP_2Se_6	44.32	13.89	0.54	0.11	0.08	0.07
$SiAs_2S_6$	46.00	15.75	0.61	1.02	0.11	0.14
$SiAs_2Se_6$	33.61	13.22	0.88	0.09	0.09	0.12
$SiAs_2Te_6$	21.11	5.85	0.57	0.22	0.03	0.05
GeP_2S_6	48.23	11.36	0.44	0.33	0.07	0.06
GeP_2Se_6	37.04	10.15	0.36	0.25	0.11	0.13
$GeAs_2S_6$	40.32	12.13	1.6	1.45	0.58	0.77
$GeAs_2Se_6$	39.65	10.75	1.13	1.21	0.41	0.18
$GeSb_2S_6$	30.36	11.09	0.08	0.04	0.03	0.06
SnP_2S_6	42.44	8.12	0.37	0.32	0.08	0.09
SnP_2Se_6	30.25	5.99	0.16	0.12	0.04	0.05
$SnAs_2S_6$	33.55	8.77	1.05	0.17	0.2	0.08
$SnAs_2Se_6$	25.41	8.20	0.85	0.3	0.3	0.16
$SnAs_2Te_6$	32.04	18.10	0.11	0.10	0.05	0.07
$SnSb_2S_6$	28.58	6.84	0.14	0.12	0.03	0.04

S8. Band structures of group-IV-V-VI monolayers

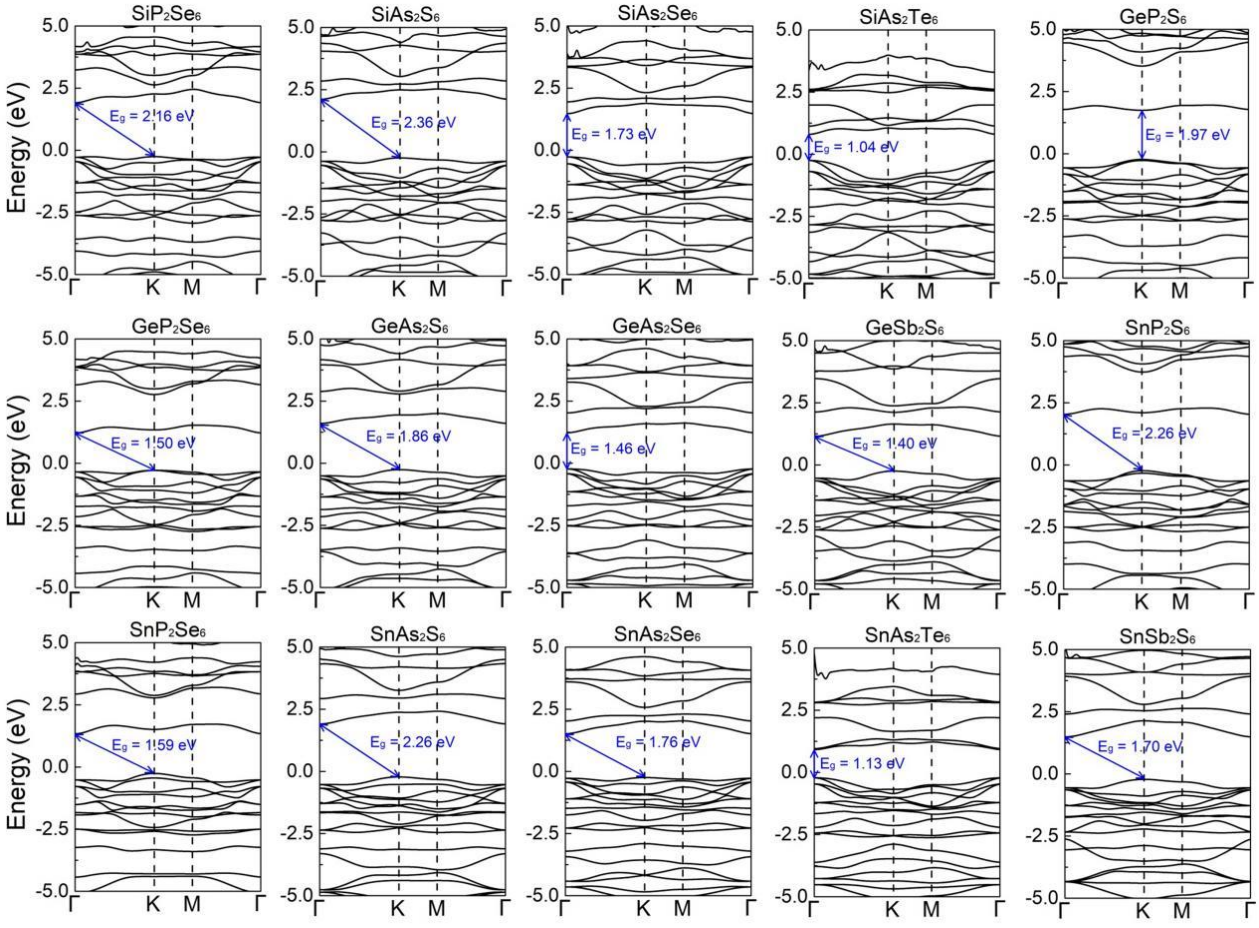

Fig. S7. Band structures of group-IV-V-VI monolayers.

S9. Phonon dispersion for the paraelectric phase of monolayer SnP_2Se_6

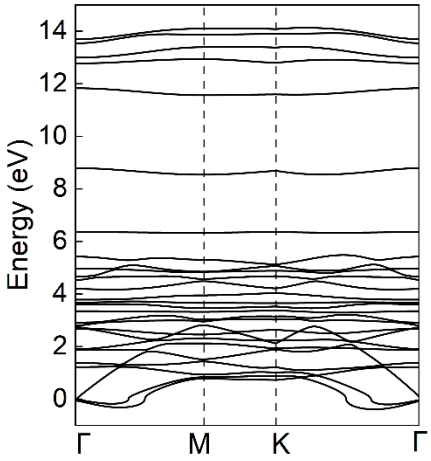

Fig. S8. Phonon dispersions for the paraelectric phase of SnP_2Se_6.

S10. Piezoelectric coefficients of $SiAs_2Te_6$

Table S2. The lattice constant a (Å), the vdW interlayer gap h (Å), elastic constants C_{11} and C_{12} (N/m) and piezoelectric coefficients d_{11}, d_{22}, d_{31} and d_{33} (pm/V) of $SiAs_2Te_6$.

$SiAs_2Te_6$	Monolayer	Bilayer	Trilayer
Point group	32	3	3
a	7.15	7.01	7.00
h	--	3.39	3.38
C_{11}	21.11	49.13	106.21
C_{22}	21.11	46.15	104.29
C_{12}	5.85	28.60	49.01
d_{11}	22.94	12.22	10.77
d_{22}	--	0.16	0.17
d_{31}	--	0.88	1.52
d_{33}	--	9.29	11.52

S11. Double-well potential versus polarization and AIMD simulations for $SiAs_2Te_6$ monolayer

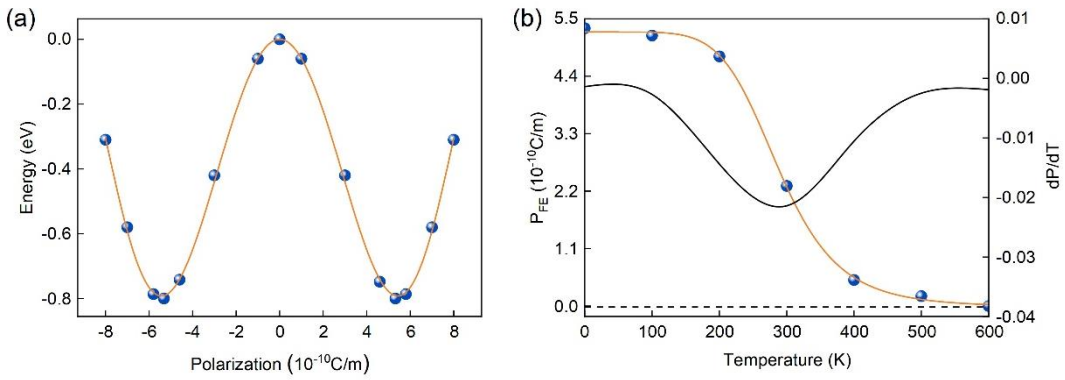

Fig. S9. (a) Double-well potential versus polarization for $SiAs_2Te_6$ monolayer. (b) Temperature dependence of polarization obtained from ab initio molecular dynamics (orange balls). Orange line is a sigmoid fit to MD results and grey line is the pyroelectric response (dP/dT) for $SiAs_2Te_6$ monolayer.